

THE OFFICIAL MAGAZINE OF THE OCEANOGRAPHY SOCIETY

Oceanography

Supplementary Materials for

Deep-Sea Volcanic Eruptions Create Unique Chemical and Biological Linkages Between the Subsurface Lithosphere and the Oceanic Hydrosphere

By Rachel L. Spietz, David A. Butterfield, Nathaniel J. Buck, Benjamin I. Larson, William W. Chadwick Jr., Sharon L. Walker, Deborah S. Kelley, and Robert M. Morris

CITATION

Spietz, R.L., D.A. Butterfield, N.J. Buck, B.I. Larson, W.W. Chadwick Jr., S.L. Walker, D.S. Kelley, and R.M. Morris. 2018. Deep-sea volcanic eruptions create unique chemical and biological linkages between the subsurface lithosphere and the oceanic hydrosphere. *Oceanography* 31(1):128–135, <https://doi.org/10.5670/oceanog.2018.120>.

DOI

<https://doi.org/10.5670/oceanog.2018.120>

COPYRIGHT

This article has been published in *Oceanography*, Volume 31, Number 1, a quarterly journal of The Oceanography Society. Copyright 2018 by The Oceanography Society. All rights reserved.

USAGE

Permission is granted to copy this article for use in teaching and research. Republication, systematic reproduction, or collective redistribution of any portion of this article by photocopy machine, reposting, or other means is permitted only with the approval of The Oceanography Society. Send all correspondence to: info@tos.org or The Oceanography Society, PO Box 1931, Rockville, MD 20849-1931, USA.

Sample Collection

Hydrothermal plumes within the caldera of Axial Seamount and over the new (April 2015) North Rift Zone (NRZ) lava flows were mapped during R/V *Thompson* rapid response cruise (TN-327, August 14–29, 2015) using a Sea-Bird Electronics 9plus CTD with integrated turbidity (optical backscatter) and oxidation-reduction potential (ORP) sensors. During tow-yos, the CTD package (which also included 24 10-liter Niskin bottles) was cycled between 10 and 200 m above the seafloor while towing along the trackline at speeds of 1–2 knots (e.g., Baker et al., 1995). Turbidity is reported here as nondimensional nephelometric turbidity units (NTU; American Public Health Association, 1985), and ΔNTU is the turbidity anomaly above the local non-plume background value. The ORP sensor responds quickly and sensitively to reduced chemical species (e.g., Fe^{2+} , HS^- , H_2) common in hydrothermal plumes (Walker et al., 2007). Real-time monitoring of the optical backscatter and ORP sensors aided in acquiring both plume and non-plume samples. The hydrothermal temperature anomaly ($\Delta\theta$) was calculated as

$$\Delta\theta = \theta - [(m_2 * \sigma_\theta^2) + (m_1 * \sigma_\theta) + m_0],$$

where θ is potential temperature, σ_θ is potential density, and m_0 , m_1 , and m_2 are constants from a polynomial regression between θ and σ_θ in hydrothermally unaffected water at, or just above, plume depths (Lupton et al., 1985). Water samples for DNA analyses for this study were obtained during CTD tow T15A-01 (August 18, 2015).

Once on deck, water samples were processed for physicochemical measurements (pH, gases, trace metals, dissolved organic matter, and nutrients) and biological samples (cells for DNA). A total of 44 water samples from plumes over the caldera, NRZ, and background were analyzed on board ship for methane and hydrogen concentration by gas chromatography (SRI GC with flame ionization and pulse discharge detectors). Water for DNA was either processed immediately once shipboard or stored at 4°C in the dark for up to eight hours until processing. To collect cells for DNA, 2 L of water were filtered onto 0.2 μm Supor polyethersulfone filters, flash frozen in liquid nitrogen, and stored at -80°C until further processing.

Small Subunit rRNA Gene Sequencing

DNA was extracted from Supor filters following previously described methods (Marshall and Morris, 2012), quantified using a Qubit fluorometer (Invitrogen, CA), concentrated using a SpeedVac (Thermo Scientific), and reconstituted in nuclease-free water (Qiagen).

The DNA was submitted to MRDNA (Stillwater, TX) for tag sequencing. At MRDNA, the V4 hypervariable region of the 16S rRNA gene was amplified using 515F and 806R primers (Apprill et al., 2015; Parada et al., 2015) with minor revisions to better amplify marine bacteria and archaea using polymerase chain reaction (PCR) conditions of an initial denaturation at 94°C for 3 minutes followed by 28 cycles of 94°C for 30 seconds, 53°C for 40 seconds, and 72°C for 1 minute, and then a final elongation step at 72°C for 5 minutes. PCR products were checked in 2% agarose gel to determine amplification success and relative intensity of amplification bands. All samples were pooled together in equal proportions, then pooled samples were purified and calibrated using AMPure XP beads. The pooled and purified PCR products were used to prepare the DNA library at MRDNA on an Illumina MiSeq using manufacturer's guidelines (Illumina, CA).

Community Analyses

Sequence data were processed by the MR DNA service facility. Their analysis pipeline has been developed to join paired ends, delete barcodes, remove sequences <150 bp or with ambiguous bases, denoise sequences, generate OTUs (based on 97% identity), remove chimeras, and finally assign taxonomy using BLASTn against a curated database derived from RDP II and NCBI (<http://rdp.cme.msu.edu>, <https://www.ncbi.nlm.nih.gov>).

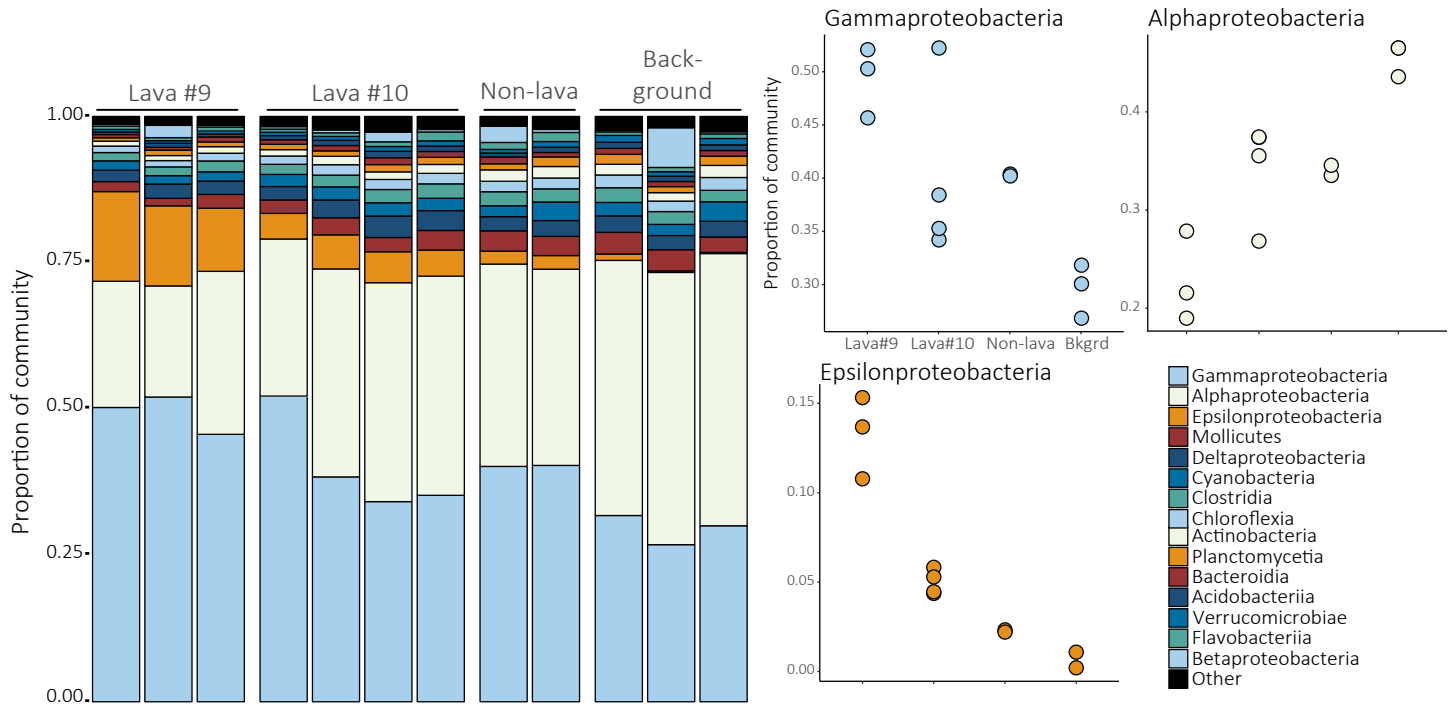
Patterns in bacterial and archaeal communities were analyzed using alpha and beta diversity measures. To minimize the effect of sampling effort, samples were rarefied to the size of the smallest sample. Alpha diversity was measured calculating the observed richness, or the number of operational taxonomic units (OTUs) present in each sample. Nonmetric multidimensional scaling (NMDS) was used to compare community composition across samples for either bacterial or archaeal taxa. A Bray-Curtis distance matrix was calculated by randomly subsampling each sample, calculating Bray-Curtis dissimilarity, and finding the average over 1,000 iterations. Analysis of similarity (ANOSIM) tests were employed to determine whether the differences in community composition were significantly larger between samples than within samples, over 999 random permutations of the data set. Lastly, taxa significantly correlated with changes in community composition across samples were identified as indicator taxa by using a similarity percentage (SIMPER) analysis. For the indicator analysis, taxa that had an average abundance of 100 sequences or more were not included because they were present, and abundant, in all 12 samples. Rather, taxa that had an average abundance between 10 and 100 sequences were considered most informative because

they were not present in all samples and thus demonstrated informative distributional patterns. All community analyses were conducted in R (The R Core Project for Statistical Computing, 2017).

REFERENCES

- American Public Health Association. 1985. *Standard Methods for the Examination of Water and Wastewater*, 16th ed., American Public Health Association, Washington, DC.
- Aprill, A., S. McNally, R. Parsons, and L. Weber. 2015. Minor revision to V4 region SSU rRNA 806R gene primer greatly increases detection of SAR11 bacterioplankton. *Aquatic Microbial Ecology* 75(2):129–137, <https://doi.org/10.3354/ame01753>.
- Baker, E.T., C.R. German, and H. Elderfield. 1995. Hydrothermal plumes over spreading-center axes: Global distributions and geological inferences. Pp. 47–71 in *Seafloor Hydrothermal Systems: Physical, Chemical, Biological, and Geological Interactions*. S. Humphris, R. Zierenberg, L. Mullineaux, and R. Thomson, eds, American Geophysical Union, Washington, DC.
- Lupton, J.E., J.R. Delaney, H.P. Johnson, and M.K. Tivey. 1985. Entrainment and vertical transport of deep-ocean water by buoyant hydrothermal plumes. *Nature* 316(6029):621–623, <https://doi.org/10.1038/316621a0>.
- Marshall, K.T., and R.M. Morris. 2012. Isolation of an aerobic sulfur oxidizer from the SUP05/Arctic96BD-19 clade. *The ISME Journal* 7(2):452–455, <https://doi.org/10.1038/ismej.2012.78>.
- Parada, A.E., D.M. Needham, and J.A. Fuhrman. 2015. Every base matters: Assessing small subunit rRNA primers for marine microbiomes with mock communities, time series and global field samples. *Environmental Microbiology* 18:1,403–1,414, <https://doi.org/10.1111/1462-2920.13023>.
- The R Core Project for Statistical Computing. 2017. R: A language and environment for statistical computing. R Foundation, Vienna, Austria, <http://www.R-project.org>.
- Walker, S.L., E.T. Baker, J.A. Resing, K. Nakamura, and P.D. McLain. 2007. A new tool for detecting hydrothermal plumes: An ORP Sensor for the PMEL MAPR. *Eos Transactions, American Geophysical Union* 88(52), Fall Meeting Supplement, Abstract V21D-0753.

A. Bacteria



B. Archaea

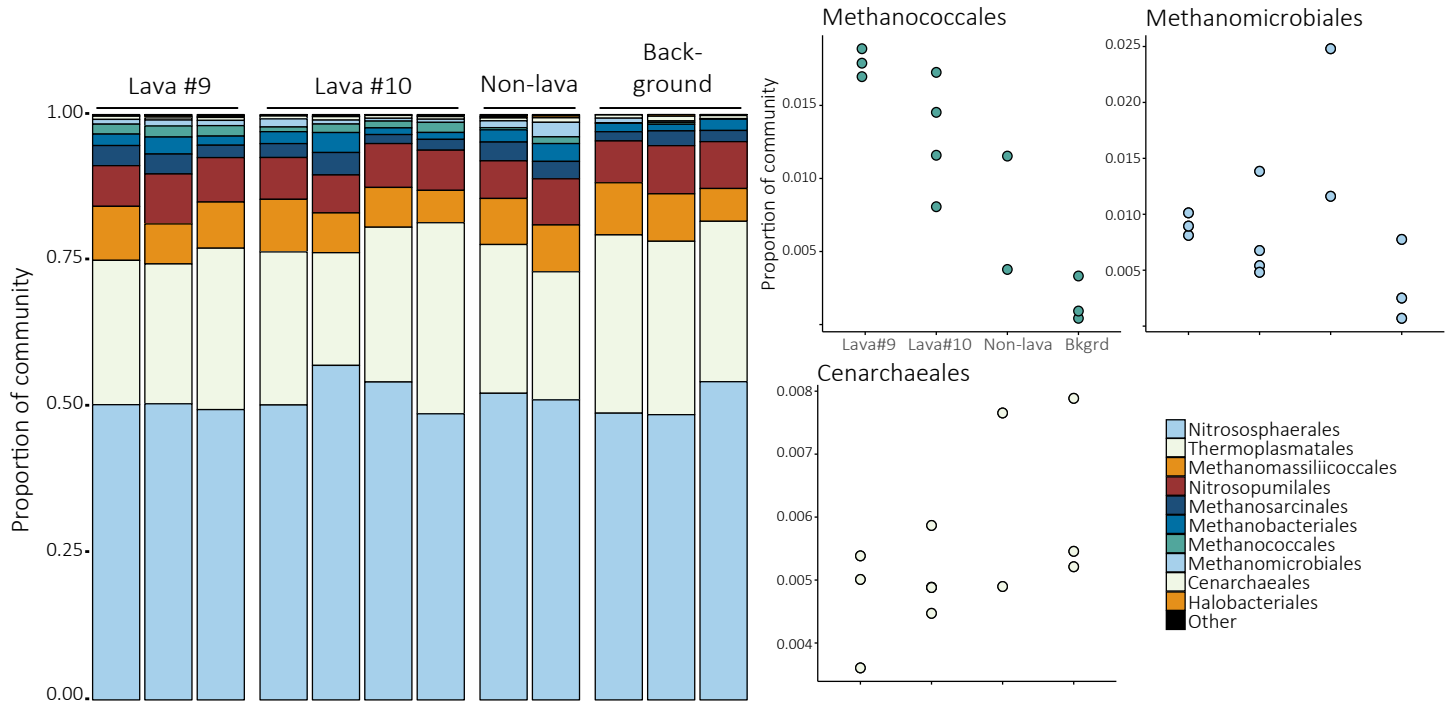


FIGURE S1. Proportions of most abundant (A) bacterial classes and (B) archaeal orders detected along the North Rift Zone of Axial Volcano following the 2015 eruption. Taxonomic groupings that represented less than 1% or 0.1% of the total community, respectively, were combined into the “other” category. Samples are ordered by decreasing turbidity anomaly, a proxy for hydrothermal circulation, from left to right. Samples are classified into four distinct sampling regions: lava flow #9, lava flow #10, non-lava, and background samples not influenced by hydrothermal activity.

TABLE S1. Correlation coefficients, adjusted R^2 , between bacterial class proportions and physicochemical parameters. High positive values indicate strong correlations while negative values indicate no correlation.

Class	ΔNTU	$\Delta\theta$	CH_4	H_2
Acidobacteriia	0.5508	0.4499	-0.1414	-0.1428
Actinobacteria	0.6284	0.3794	0.3910	0.1374
Alphaproteobacteria	0.7402	0.7838	0.1296	0.0332
Bacteroidia	0.5387	0.0611	0.0160	-0.0835
Betaproteobacteria	-0.0493	-0.0304	0.0066	-0.0433
Chloroflexia	0.7930	0.6637	0.1600	-0.0355
Clostridia	0.6528	0.1965	-0.1338	0.1546
Cyanobacteria	0.3612	0.3691	0.1003	-0.1214
Deltaproteobacteria	0.1770	-0.0346	0.1859	-0.1362
Epsilonproteobacteria	0.9594	0.6732	0.3879	-0.0730
Flavobacteriia	0.0821	-0.0848	-0.0357	0.2003
Gammaproteobacteria	0.5717	0.6325	0.0127	0.1058
Mollicutes	0.6784	0.3461	0.1814	0.0539
Other	0.4872	0.3750	-0.1329	-0.1411
Planctomycetia	0.4575	0.4545	0.1345	0.0702
Verrucomicrobiae	0.5486	0.6565	0.1226	0.0277

ΔNTU = turbidity anomaly in nephelometric turbidity units; $\Delta\theta$ = temperature anomaly

TABLE S2. Correlation coefficients, adjusted R^2 , between archaeal order proportions and physicochemical parameters. High positive values indicate strong correlations while negative values indicate no correlation.

Order	ΔNTU	$\Delta\theta$	CH_4	H_2
Cenarchaeales	0.1454	-0.0152	-0.1397	0.0575
Halobacteriales	-0.0933	-0.0727	-0.0257	-0.0847
Methanobacteriales	-0.0890	0.0565	-0.0909	0.1421
Methanococcales	0.5515	0.8154	0.6264	0.1378
Methanomassiliicoccales	-0.0977	-0.0922	-0.1190	0.2300
Methanomicrobiales	-0.0964	0.1097	-0.1351	0.0183
Methanosarcinales	-0.0501	0.1486	-0.0456	0.0749
Nitrosopumilales	-0.0372	-0.0986	-0.0349	-0.1384
Nitrososphaerales	-0.0421	-0.1000	0.0032	-0.1348
Other (less than 0.1%)	0.2628	0.5083	0.0925	-0.1243
Thermoplasmatales	-0.0836	0.1441	0.0157	-0.0089

ΔNTU = turbidity anomaly in nephelometric turbidity units; $\Delta\theta$ = temperature anomaly